ANSTO/E706

ANSTO/E706

ansto

HIGH PURITY LIQUID PHASE EPITAXIAL GALLIUM ARSENIDE NUCLEAR RADIATION DETECTOR

by

DIMITRI ALEXIEV
and
K.S.A. BUTCHER

NOVEMBER 1991

REPORT E

ISBN 642 59925 4
ISSN 1030-7745

AUSTRALIAN NUCLEAR SCIENCE AND TECHNOLOGY ORGANISATION

LUCAS HEIGHTS RESEARCH LABORATORIES

HIGH PURITY LIQUID PHASE EPITAXIAL GALLIUM ARSENIDE NUCLEAR RADIATION DETECTOR

by

DIMITRI ALEXIEV
and
K.S.A. BUTCHER

ABSTRACT

Surface barrier radiation detector made from high purity liquid phase epitaxial gallium arsenide wafers have been operated as X- and γ-ray detectors at various operating temperatures. Low energy isotopes are resolved including ^{241}Am at 40°C and the higher gamma energies of ^{235}U at -80°C.

National Library of Australia card number and ISBN 0 642 59925 4

The following descriptions have been selected from the INIS Thesaurus to describe the subject content of this report for information retrieval purposes. For further details please refer to IAEA-INIS-12 (INIS: Manual for Indexing) and IAEA-INIS-13 (INIS: Thesaurus) published in Vienna by the International Atomic Energy Agency.

Americium 241; Ansto; crystal growth; epitaxy; experimental data; gallium arsenides; gamma detection; leakage current; performance testing; spectroscopy; surface barrier detectors; temperature dependence; uranium 235; uses; X-ray detection.

EDITORIAL NOTE

The Australian Nuclear Science and Technology Organisation replaced the Australian Atomic Energy Commission on 27 April 1987. Reports issued after April 1987 have the prefix ANSTO with no change of the symbol (E, M, S or C) or numbering sequence.

CONTENTS

		Page No
1.	INTRODUCTION	1
2.	PRINCIPLES OF OPERATION	2
3.	DIODE FABRICATION AND ELECTRICAL MEASUREMENTS	4
	3.1 Electrical Measurements	6
4.	RADIATION MEASUREMENTS	7
5.	CONCLUSION	8

1. Introduction

Wide bandgap compound semiconductor materials are potentially useful as room temperature (~300K) nuclear radiation detectors whereas elemental semiconductors such as silicon and germanium must be cooled to liquid nitrogen temperatures (77K) before operation, thereby restricting their suitability for many applications.

High atomic number (Z) semiconductor materials such as GaAs (Z_{av} = 32) have been investigated by Harding et al (1960)[1]; Dearnaley and Northrop (1963)[2]; Mayer (1962)[3] and Kobayaski et al (1966)[4] as α-particle detectors; the resolution of such (Kobayaski et al[4]) devices was 420 KeV FWHM and no evidence was noted of either X-ray or γ-ray photopeaks. The poor resolution was mainly attributed to carrier trapping due to poor crystallinity of the material. Eberhardt et al (1971)[5]; Gibbons and Howes (1972)[6] and Kobayaski et al (1972)[7] showed that liquid phase epitaxy can produce GaAs with excellent charge collection characteristics. Epitaxial layers were thin ranging mostly from 30 to 60 μm which in turn would be further reduced in thickness after chemical etching. The publication by Eberhardt et al (1971)[5], described excellent X-and γ-ray resolution (2.95 KeV FWHM for the 122 KeV Co^{57} γ line) despite the high leakage current (I_R) of 1 x 10^{-9}A at 100 V_R bars, near full depletion of a ~ 60 μm epitaxial n-layer at room temperature.

This paper describes work aimed at further investigating liquid phase epitaxial Gallium Arsenide for application as nuclear radiation detectors in biomedical probes, X-ray and low energy γ-ray detectors, X-ray fluorescence radiation detectors and U^{235} safeguards applications.

The material used for device construction was grown and prepared at the Australian Nuclear Science and Technology Organisation and details of the growth method will be published later. The LPE layers were mostly n-type with a preferred free carrier concentration between 2×10^{13} and 2×10^{14} cm^{-3}. Epitaxial layer thickness up to 220 μm were examined. Operating temperatures of between 130K and 340K were used for the better (low I_R) devices.

2 Principles of Operation

A charged particle entering a surface barrier detector produces one free electron-hole pair for each 4.51 eV of energy absorbed in GaAs (Wittry et al (1965))[8] (the equivalent figures are 3.6 eV Si and 2.9 eV for Ge). The particle is brought to rest almost instantaneously in a time between 10^{-12} to 10^{-11}s, losing almost all the energy in the production of low energy electrons by impact ionisation. γ-rays do not quite fit this pattern; they produce at each interaction an energetic electron, either by the photoelectric or Compton process. These may then be considered similar to primary bombarding particles though not originating at the surface of the detector. Secondary electrons, in turn, lose their energy rapidly by further impact ionisation until their remaining kinetic energy is insufficient to excite an electron-hole pair. The number of electron-hole pairs produced is proportional to the energy lost; therefore detectors can give an excellent linear relationship between the size of the current pulse generated and the particle energy provided the depletion depth exceeds the range of the full energy exchange process. Clearly the field strength in the depletion layer must be sufficient to separate the charge carriers before they recombine (ORTEC (1976))[9].

If all the deposited energy is used in ionisation then no fluctuations occur in the number of carriers produced by ionising radiation of a given energy. However, energy may be dissipated by thermal heating of the lattice. If the probability of an ionising event is low compared with that of the thermal process then Poisson statistics apply and the R.M.S. fluctuation $\langle n \rangle$ in the number of pair production is:

$$\langle n \rangle = \sqrt{\frac{E}{\epsilon}}$$

where E = energy absorbed by the detector

ϵ = average energy required for production of electron-hole pair.

However, in a semiconductor detector, this simple analysis does not hold. Energy losses by the electron shower produced by an ionising process (γ-ray or particle) are of three types (Goulding (1966))[10]:

I. The promotion of an electron in the lattice to the conduction band. The remainder of the energy is shared between the incident electron, the secondary electron and the secondary hole.

II. Energy loss by interaction with the lattice itself, exciting the optical and accoustical modes of vibration.

III. Thermal losses to the lattice by the low energy electrons at the end of the shower process which have insufficient energy for secondary ionisation.

To allow for these possible competing processes, the Fano factor F, is introduced. If the observed R.M.S. spread is n_o,

$$n_o^2 = F\langle n \rangle^2$$

A further relevant observation is that the reverse current (I_R) across a p-n junction (detector) has two inherent components (Taylor (1963))[11]:

I. The junction generation current, whereby electrons and holes produced in the depletion layer are removed by the applied field, in the same way as those produced by ionising radiation.

II. Surface leakage is thought to have components due to the generation of charge carriers formed at the surface that have impaired valences electrons or "dangling bonds" (Lindmayer and Wrigley (1979))[12] Such surfaces will be sensitive to chemisorption of some foreign species (Pearton et al (1984)[13] and Nelson et al (1980))[14].

3. Diode Fabrication and Electrical Measurements

Detectors were constructed by first cleaving 5 mm square sections from selected LPE wafers. These were cleaned by ultrasonic agitation in xylene, followed by methanol and ultimately in 18 $M\Omega H_2O$. An ohmic contact was made by evaporating Al onto the substrate and the rectifying surface barrier p contact by evaporating Au (~ 10 μm thickness) to a freshly etched surface. The surface of the epitaxy was not polished, only etched for 30 sec in 50°C $H_2SO_4:H_2O_2:H_2$) = 3:1:1, followed by displacive rinsing in 18 $M\Omega H_2O$. A schematic of the radiation detector is shown in Fig.1.

The radiation detector is completed by attaching the substrate side (ohmic contact) to an aluminium holder with colloidal silver paste. The metal barrier contact is made by connecting a thin palladium wire with silver bonding cement to a teflon feed-through barb. The complete detector is shown in photograph 1.

After construction, all detectors were tested using standard diode characterisation techniques such as I-V, C-V and spectral response at various temperatures. This was achieved by placing the detectors into a liquid nitrogen (ℓN_2) cryostat with the barrier contact connected through a high quality, low capacity feed-through connector supplied by Ceramaseal (USA) to an AC coupled, EG&G charge sensitive preamplifier using an uncooled front stage FET.

The ambient electrical noise level of the system with zero capacity at the input was found to be 1.8 KeV FWHM on an equivalent energy of an Am^{241} line when calibrated with an LPE-GaAs detector and a pulser. Spectroscopic examination of various isotopes showed that the device produced no contributing noise factor to the resolution of the system. This was evident when a pulser line was introduced into an accumulating spectrum. However, it will be appreciated that the preamplifier noise is primarily dependent on the input capacitance (detector, feed-through connector, feedback resistor capacitance and feedback capacitor) and the input field effect transistor (FET). Typical input capacitance specification is given by ORTEC as $\leq$ .03 keV/pf FWHM (Ge) slope.

Spectral resolution can be improved by DC coupling of the device providing $I_R < 10^{-10}$A and by peltier cooling selected FET's in the input stage of the preamplifier.

3.1 *Electrical Measurements*

Fig.2 shows a range of leakage currents (I_R) with reverse bias (V_R) at various temperatures. The first observation is that there is a wide variation in leakage currents between diodes prepared in a similar fashion. The second is that, as the temperature of the device is decreased, the leakage current reduces from approximately 10^{-9}A to less than 10^{-13}A, at the limit of the measuring equipment, at a given bias.

The higher I_R at elevated temperatures can be explained by a combination of the following:

I. Surface leakage currents which can be expected as a resistive function of (V_R);

II. Bulk generated currents, such as localised generating centres at the substrate-epitaxy interface as suggested by Eberhardt et al (1971)[5].

However, it was found that at lower bias voltages the exponential temperature coefficient of I_R is close to the expected bulk generation currents in GaAs, $Eg/2 \simeq 0.7$ eV, whereas at lower device temperatures and at high bias voltages, the temperature coefficient becomes much lower. This leads one to conclude that surface leakage currents are dominant at higher bias voltages and at elevated temperatures (~ 20 to 40°C). It is also clear that surface preparation and surface passivation must play an important part in successful and stable room temperature operating devices.

In general, devices with less than 3×10^{-9}A at near full depletion voltages showed good spectral resolution. There was no evidence of multi-peaking and polarisation as noted by Tavendale et al (1972)[15]. This is usually caused by uneven depletion into the epitaxy-interface layer, due to non homogeneity of the material. This results in charge sharing and

ultimately bias dependency on pulse height response. The polarisation noted by Tavendale et al (1972)[15] was deduced as a major deep level trap; by introducing an infrared (IR) source in the vicinity of the detector, the spectral resolution improved as the deep level trap was filled, preventing further charge trapping during spectral measurements.

4. Radiation Measurements

All devices constructed were first tested for I-V characteristics, those which had leakage currents less than 5×10^{-9}A at about 100V bias were tested for spectral response at various temperatures. One of the better devices was used to resolve Am^{241}. The 17.74 KeV X-ray and 59.45 KeV γ-line were compared to a pulser line set at equivalent 70 KeV energy. Results are shown in Table 1.

It will be noted from Table 1 that the detector contributed little if anything to the overall limitations in resolution. Best results were obtained at -80°C, deliberately chosen since such a temperature can be easily obtained with a triple stack peltier cell. The τ_{RC} shaping time constant was optimised at 4 μS, however, 2 μS can also be used with little noted difference in resolution. When the device was operated at +40°C the spectral quality and resolution (2.8 KeV, FWHM) were maintained indicating that the device can be used in medical probes such as in cancer detection using I^{125} tagged monoclonal antibodies.

Figure 3 shows a typical Am^{241} spectrum at room temperature (300K)

4 shows a typical Co^{57} with the 122 KeV line clearly resolved

5 shows U^{235}

6 shows U^{235} and γ-ray background of Cs^{137}

Both Figures 5 and 6 are of interest in nuclear fuel safeguards inspection. A 36 gms sample of 90% enriched U^{235} was counted for 80 minutes (Figure 5). Then 20 mc Cs^{137} was similarly counted to simulate a fuel element's γ background activity. The 185 KeV U^{235} line is clearly resolved in Figure 5. In Figure 6 the overall spectral quality is reduced as expected, but still resolves the 185 KeV line.

5. Conclusion

When comparing the device properties of different types of LPE layers, i.e. as grown in silica, thermally annealed or neutron transmutation doped (NTD) (details to be published), little difference was noted. In all devices examined, I_R was the dominant variable and determined whether a device was useful as a spectrometer.

Devices made from NTD material showed no residual activity when counted over 4 hours with the amplifier gain set to Am^{241} energies.

In general, it was found that epitaxial GaAs can be used to fabricate a variety of room temperature X-and γ-ray spectrometers, noting that surface passivation must be an important sequence in their preparation.

Acknowledgement

We thank Dr J.W. Boldeman for his keen interest and support in this work and Mrs M. Edmondson for preparing the manuscript.

References

[1] W.R. Harding, C. Hilsum, M.E. Monchaster, D.C. Northrop and O. Simpson, Nature 187, (1960) 405.

[2] G. Dearnaley and D.C. Northrop, 'Semiconductor Counters for Nuclear Radiations (E. and F.N. Spon. London, 1963).

[3] J.W. Mayer, Nucleonics, 20, (1962) 60.

[4] T. Kobayaski and S. Takayanagi, Nucl. Inst. Meth. 44, (1966) 145.

[5] J.E. Eberhardt, R.D. Ryan and A.J. Tavendale, Nucl. Inst. Meth. 94, 463-476 (1971); App. Phys. Letters, 17, (1970) 427.

[6] P.E. Gibbons and J.H. Howes, IEEE Trans. Nucl. Sci. NS-19, (1972) 353.

[7] T. Kobayaski, T. Sugita, M. Koyama and Takayanagi, S., IEEE Trans. Nucl. Sci. NS-19, (1972) 324.

[8] D.B. Wittry and D.F. Kyser, J. Appl. Phys. 36, (1965) 1387.

[9] ORTEC "Instruments for Research" Catalog 1002 (1970-71).

[10] F.S. Goulding, Nucl. Instr. Meth. 43, (1966) 1.

[11] J.M. Taylor, "Semiconductor Particle Detectors", Lond. Butterworth (1963).

[12] J. Lindmayer and C.Y. Wrigley, "Fundamentals of Semiconductor Devices", Krieger Pub. Co. (1979).

[13] S.J. Pearton, E.E. Haller and A.G. Elliot, Appl. Phys. Lett. 44, (1984) 7.

[14] R.J. Nelson, J.S. Williams, H.J. Leamy, B. Miller, H.C. Casey, B.A. Parkinson and A. Heller, Appl. Phys. Lett. 36, (1980) 76.

[15] A.J. Tavendale and E.M. Lawson, IEEE Trans. Nucl. Sci. NS-19, (1972) 318.

TABLE 1

Enclosure	Temperature of Device	Leakage Current (A)	Resolution, FWHM (Kev), Am^{241}		Pulser, FWHM (KeV) [70KeV line]
			17.74 KeV X-ray	59.45 KeV γ-line	
N_2, gas	40°C	2×10^{-9}	2.5	3.0	2.6
N_2, gas	R/T	5.2×10^{-10}	2.2	2.7	2.5
Vacuum	R/T	4.2×10^{-10}	2.1	2.35	2.25
Vacuum	0°C	1.5×10^{-10}	1.97	2.2	2.09
Vacuum	-80°C	3×10^{-12}	1.93	2.1	1.98

Detector data: C_j = 10pf at 100V bias

Epitaxial layer = ~ 120 μm

Shaping time(τ_{RC}) = 4 μS

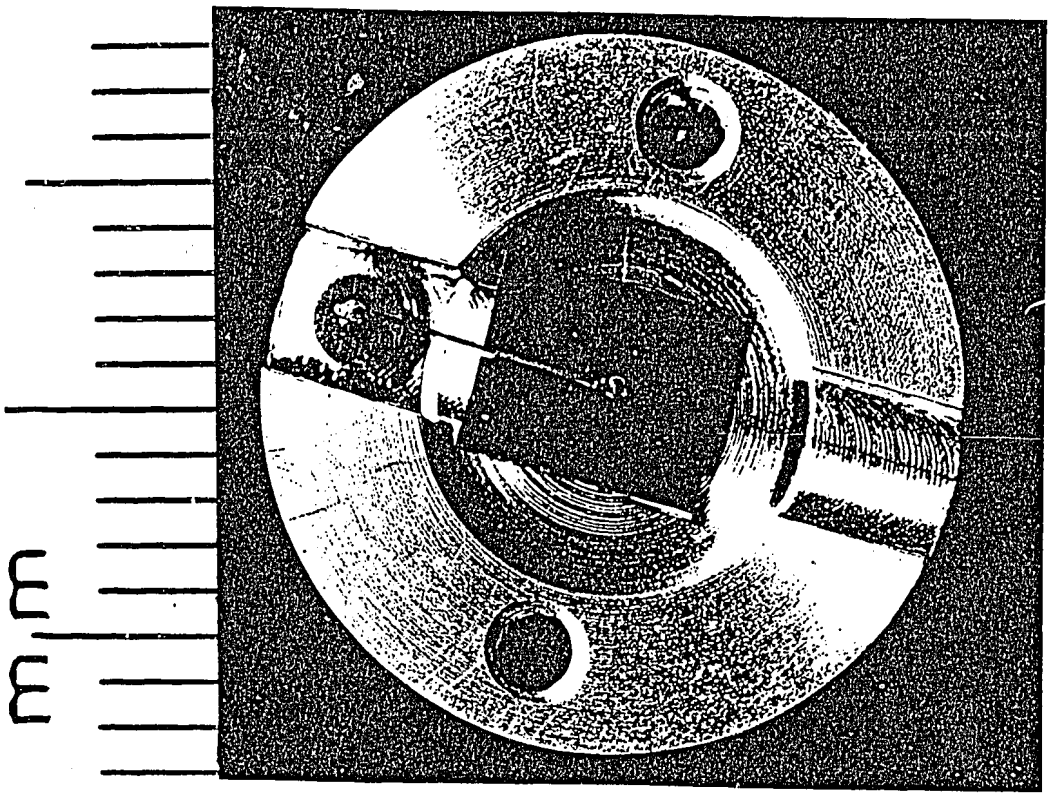

Photograph 1: Complete surface barrier radiation detector mounted in an aluminium holder. [Note: holder design beam adopted from Gibbons and Howes (1972)[6]].

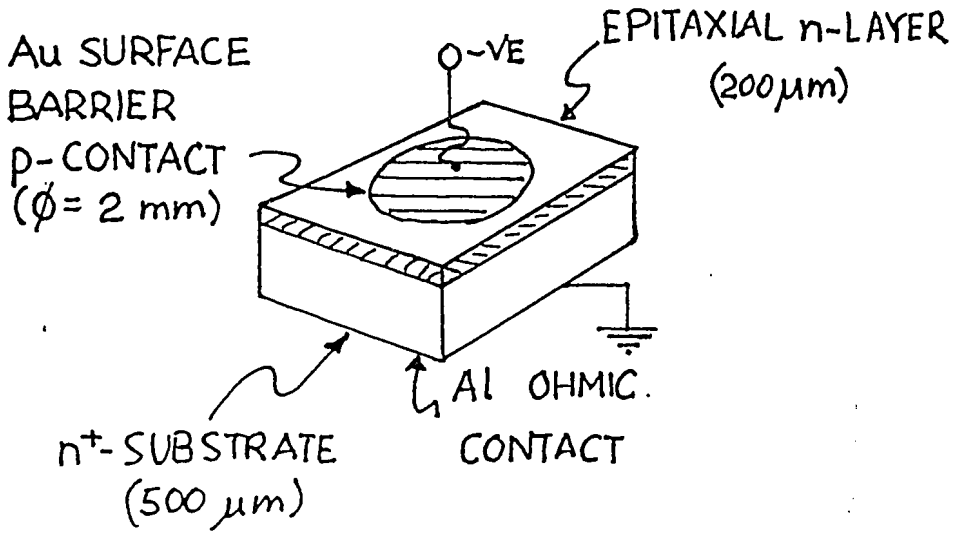

Figure 1. Schematic of a nuclear radiation detector

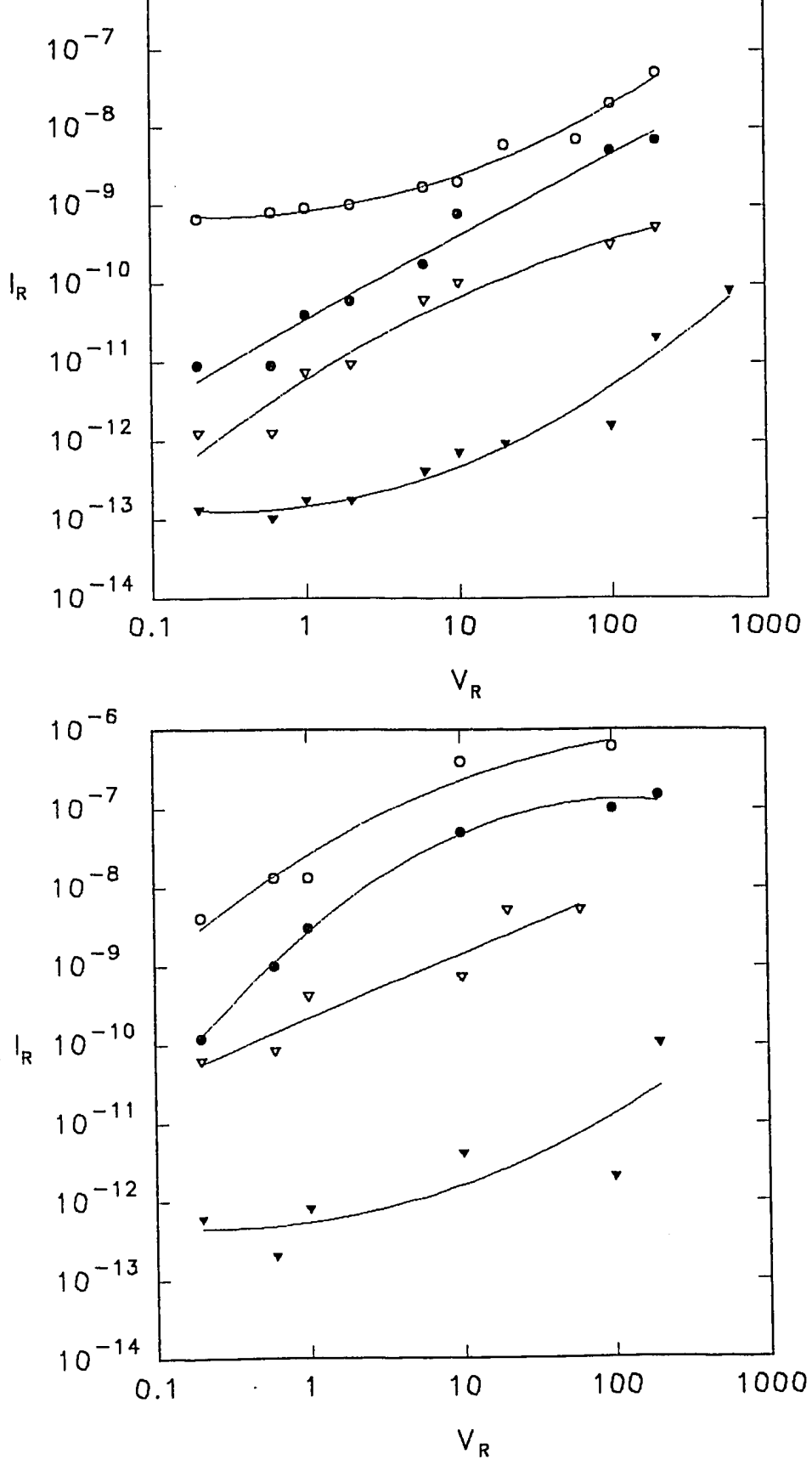

Fig. 2 - Shows I_R versus V_R for two diodes at various temperatures
o = 340K, ● = 300K, ▽ = 280K and ▼ = 220K
(Barrier: 1.5 mm Ø Au, ohmic contact: Al).

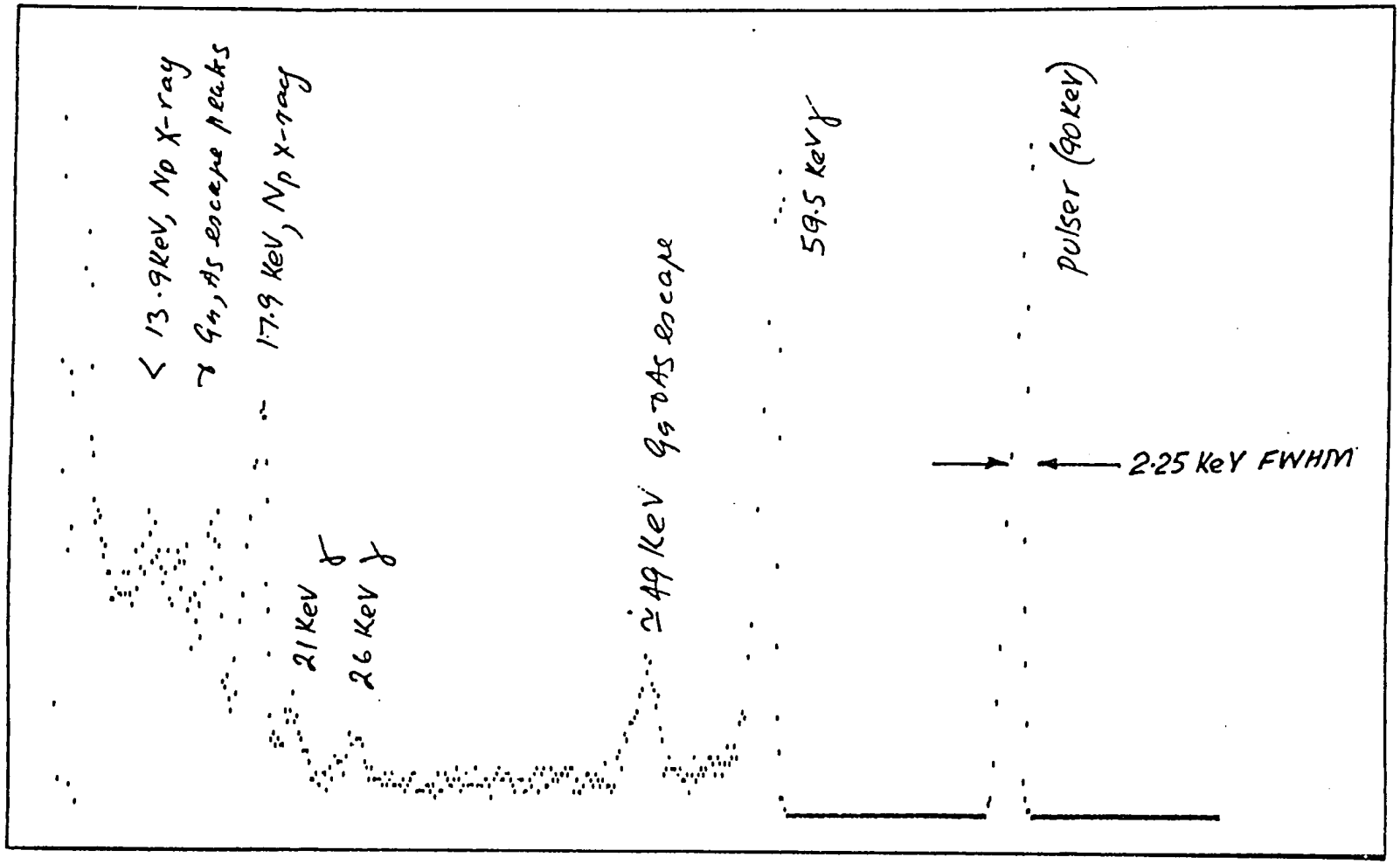

Figure 3 - Spectrum of Am^{241} Detector:

V_R = 100V, $I_R \simeq 4 \times 10^{-10}$A.

Epitaxial layer thickness: 120μm.

Operation: room temperature.

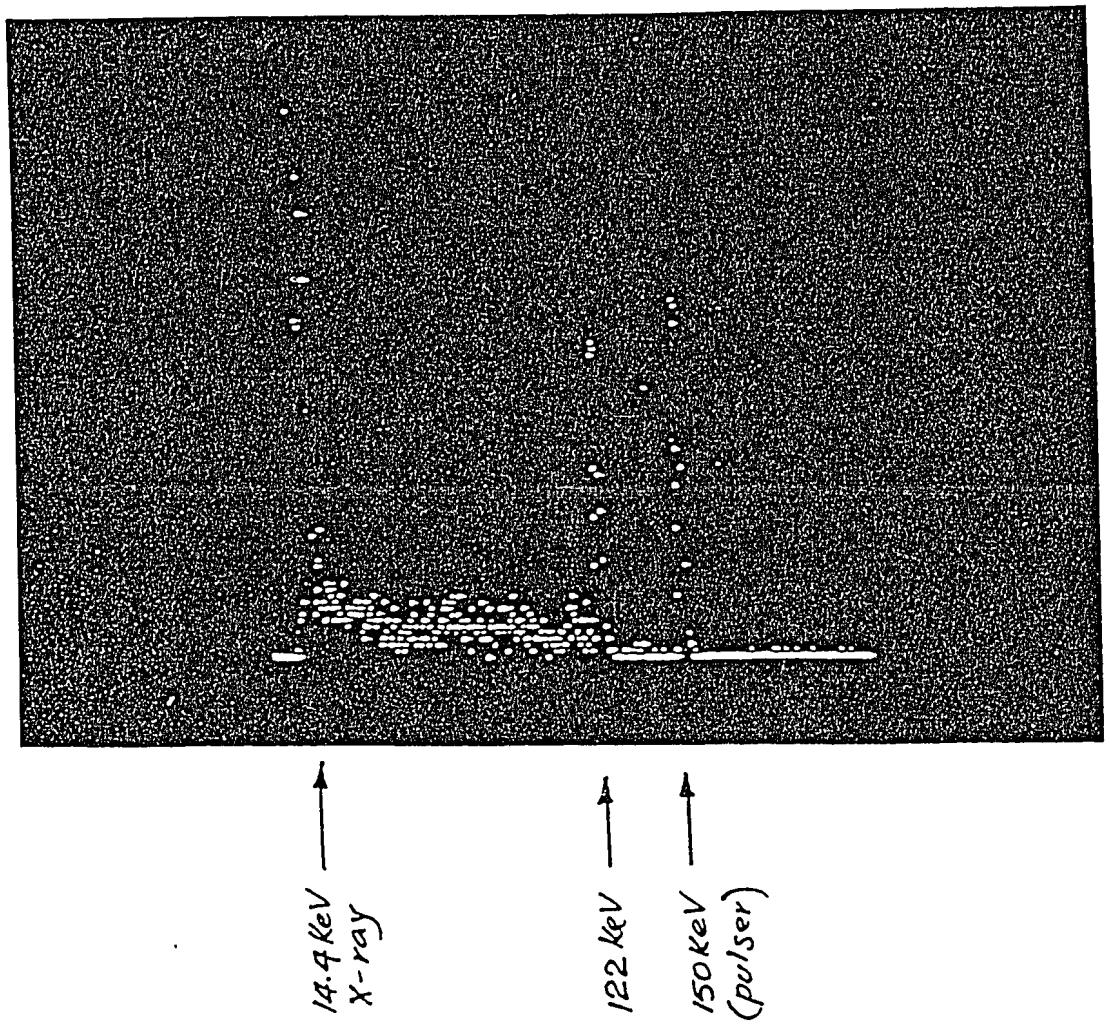

Figure 4 - Spectrum of Co^{57}, resolving the 122 keV γ line; a pulser line with an equivalent energy of 150 keV is used for resolution measurements.

Detector: 1.5 m ϕ barrier

180 μm thick epitaxial layer

V_R: 120 V, I_R = $\simeq$ 1 x 10^{-9} A, at room

room temperature

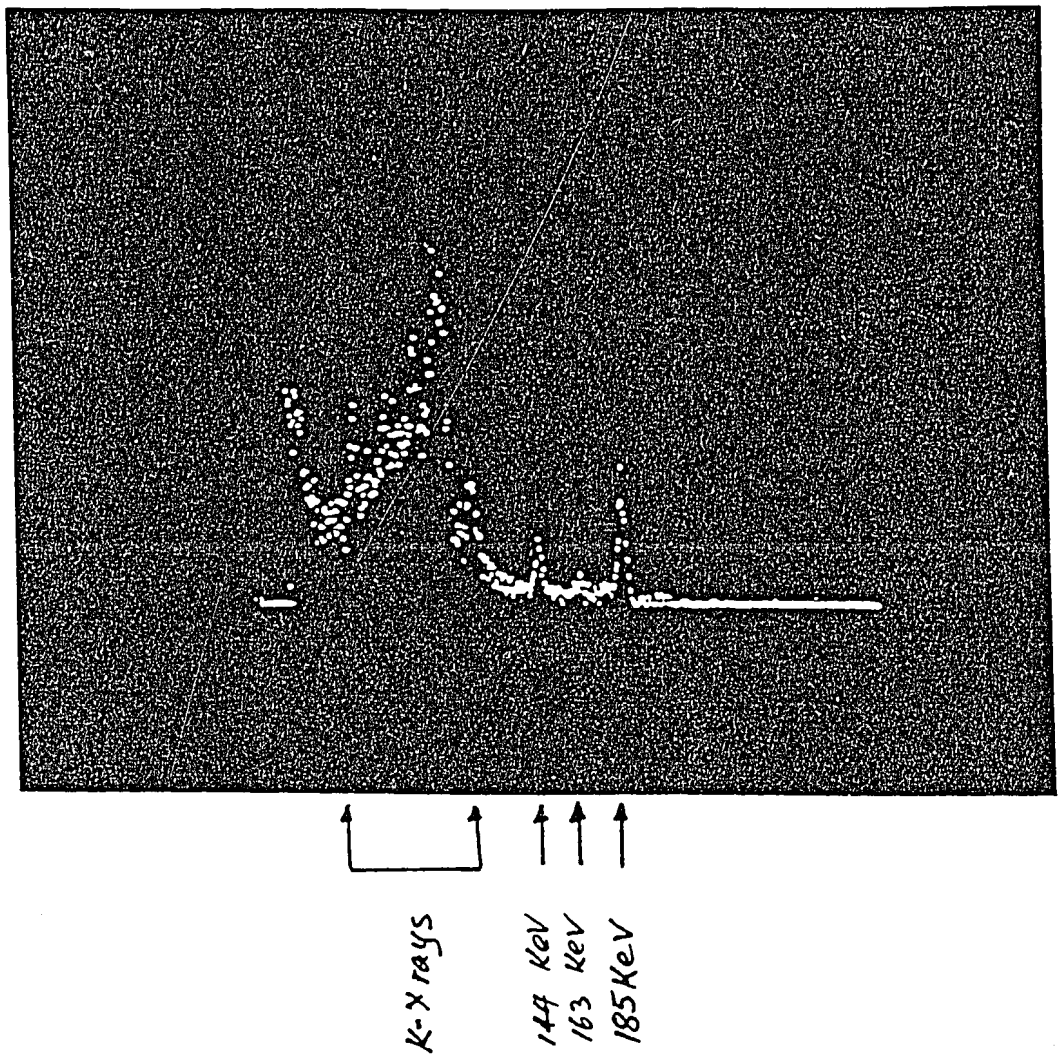

Figure 5 - Spectrum of U^{235}, clearly resolving the 185 KeV γ line and lower energies

Detector: 1 mm ϕ barrier

300 μm thick epitaxial layer

V_R: 300 V, $I_R < 10^{-13}$ A, cooled to -80°C

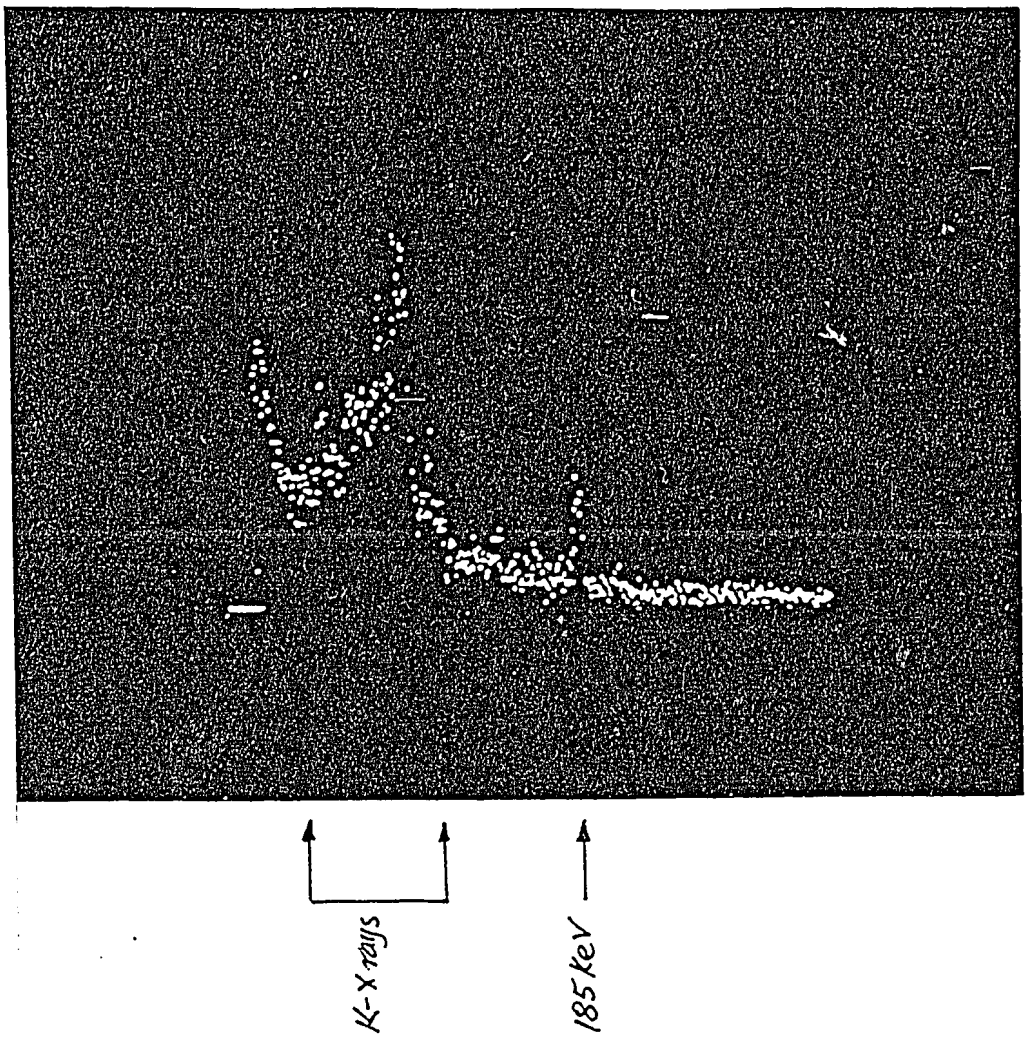

Figure 6 - Spectrum of U^{235} + Cs^{137}, shows 185 KeV γ line and γ -ray background of Cs^{137}

Detector as in Figure 5